



Plasmon-Enhanced Sensitization of Solar Cells with Dyes

G. Omarova,* E. Seliverstova,* A. Sadykova and N. Ibrayev

Abstract

The effect of localised plasmon resonance (LPR) of core@shell nanoparticles (Ag@TiO₂ NPs) and Förster resonance energy transfer (FRET) between dyes in dye-sensitized solar cell (DSSC) was investigated. It is shown that FRET is efficiently realized in donor-acceptor (DA) pairs based on Rhodamine 6G (Rh6G) and polymethine dyes (PD1 and PD2) adsorbed onto TiO₂ semiconductor films. The energy transfer efficiency (E_{ET}) is higher for the Rh6G–PD2 pair ($E_{ET}=0.55$) compared to the PD1–PD2 pair ($E_{ET}=0.21$). The incorporation of Ag@TiO₂ NPs contributes to an increase of FRET rate constant k_{ET} . The largest increase of k_{ET} (5.6-fold) is observed for the PD1–PD2 pair, whereas the increase of k_{ET} is equal to 1.7 for the Rh6G–PD2 pair. It is shown that the combined use of LPR of Ag@TiO₂ NPs and FRET leads to a significant increase of solar cell efficiency. This efficiency enhancement is attributed not only to improved light harvesting but also to the plasmon-enhanced FRET efficiency. Additionally, an improvement of the electrophysical characteristics of the cells cannot be ruled out. The obtained results demonstrate the potential of the combined application of LPR of metal NPs and FRET to enhance the performance of solar cells.

Keywords: Solar cell; Dye sensitization; Core@shell nanoparticles; Plasmon; Förster resonance energy transfer; Efficiency.

Received: 17 March 2025; Revised: 07 April 2025; Accepted: 17 May 2025.

Article type: Research article.

1. Introduction

At present, humanity is facing a continuous growth of electricity consumption that necessitates the search for efficient sources of electric power. At the same time, environmental concerns impose additional requirements on energy technologies, demanding their minimal carbon footprint both at the production stage and during operation. In this context, the use of renewable energy sources is of particular relevance. Solar energy reaching the Earth's surface has a significant energy potential, estimated at 1.75×10^7 W, making the optimization of methods for its conversion into electricity a priority for researchers. At the same time, both the optimization of traditional silicon photovoltaic cells and the development of third-generation solar cells remain relevant. Among the latter, dye-sensitized solar cells (DSSC) are of particular interest. In DSSCs, dyes act as intermediaries in the process of converting photon energy into electric current.

One of the approaches to increase the DSSC efficiency is

the application of Förster resonance energy transfer (FRET).

In particular, it was previously shown that FRET between two metal-free organic dyes leads to an almost twofold increase in the DSSC efficiency.^[1-3] This effect is attributed to the enhanced photosensitivity of the cell and the growth of the number of generated charge carriers on the surface between the titanium dioxide (TiO₂) semiconductor layer and the dye. The authors of Ref.^[4] have also used FRET from donor metal-free molecules to the N719 ruthenium dye in DSSCs based on zinc oxide (ZnO) or nickel oxide (NiO) with the addition of carbon dots (Cdots). It was shown that FRET enhances light harvesting in the solar cell, while Cdots improve dye adsorption and prevent charge recombination in the semiconductor. In organic solar cells, the use of FRET resulted in reduced recombination of electron-hole pairs in the donor part of the molecule, leading to an increase in the efficiency of the solar cell.^[5] It was shown that FRET can be beneficial in ternary blend organic solar cells, contributing to efficient charge generation, reduced energy loss, increased photon harvesting, and optimized exciton dissociation at the interface.^[6] Also, the radiationless electron excitation energy transfer was used in solar concentrators to reduce optical losses in such systems and to extend their absorption range.^[7]

Institute of Molecular Nanophotonics, Buketov Karaganda University, Karaganda, 100024, Kazakhstan

*Email: imnph@mail.ksu.kz (E. Seliverstova);

guldenserikovna@mail.ru (G. Omarova)

⁹⁾ The application of energy transfer between indium phosphide/zinc sulfide (InP/ZnS) quantum dots allowed Roy *et al.*^[10] to develop environmentally friendly assembly in light-emitting diodes.

To increase the FRET rate, the phenomenon of localized plasmon resonance (LPR) of metal nanoparticles (NPs) can be used. In this case, the efficiency of the plasmon effect and the energy transfer rate can be controlled both by adjusting the distance between the interacting particles and by tuning the overlap integral of the absorption and fluorescence spectra in the donor-acceptor pair and with plasmon NPs. Thus, Plasmon-enhanced energy transfer was studied in donor-acceptor pairs with different energy transfer efficiencies in Ibrayev *et al.*^[11] It was shown that the greatest influence of the plasmon effect on the fluorescence intensity of the dye film is observed at a distance of ~6 nm from the silver island film. The plasmon enhancement of energy transfer was more pronounced for pairs with initially low energy transfer efficiency. Also, the LPR of metal NPs can be applied to increase the Förster radius in a donor-acceptor pair that is important for such applications where energy transfer is used as a spectroscopic ruler.^[12]

Thus, FRET and the plasmon effect are effective strategies for increasing the efficiency of different types of photovoltaic devices. However, the question of their simultaneous effect on the performance of solar cells is still open, and many compound classes have not yet been studied in this context. In the present work, the plasmon effect of core@shell Ag@TiO₂ NPs on FRET in donor-acceptor pairs based on rhodamine and polymethine dyes (PDs), as well as in a pair of cationic indopolycarbocyanines adsorbed on the surface of TiO₂ semiconductor films, was studied. The conditions for efficient spectral sensitization of TiO₂ under the influence of LPR were considered. The combination of these factors offers a promising strategy to improve the performance of solar cells utilizing organic dyes. The choice of dyes is driven by the fact that metal-free organic dyes are a more accessible, environmentally friendly, and cost-effective alternative to the

metal compounds currently used in solar cells. The main advantage of such compounds is their tunable absorption and electrochemical properties, which can be tailored through appropriate synthesis strategies. The combined application of LPR of metal NPs and FRET in such systems may significantly expand the potential of metal-free sensitizers in DSSC.

2. Experimental section

Rhodamine 6G (99%), titanium (IV) oxide (21 nm, anatase, 99.7%), ethylene glycol (99.8%), poly(glycerol sebacate) (PGS), AgNO₃ (>99.8%), acetone (99.5%), tetraisopropyl orthotitanate (>99%), propanol-2 (≥99.5%), FTO substrates (1.5×1 cm, 7 Ω/cm²) were purchased from Sigma Aldrich. Polyvinylpyrrolidone-10000 was obtained from AppliChem. PDs (PD1 and PD2) were synthesized in the Institute of Organic Chemistry of National Academy of Sciences of Ukraine (Ukraine).

The xanthene dye Rhodamine 6G (Rh6G) and functionalized dye PD1 were chosen as energy donors (Fig. 1). These dyes absorb light in a similar spectral region, but differ significantly in the fluorescence quantum yield. The presence of hydroxyl functional groups in the structure of PD1 will allow it to adsorb efficiently on the surface of the semiconductor film. A single acceptor, the non-functionalized dye PD2, was used for both donors. All selected dyes absorb in the green and red regions of the visible spectrum. As is well known, the visible region accounts for ~43% of solar radiation, making it relevant to search for sensitizers that absorb in this region of the spectrum.^[13]

In addition, alignment of the highest occupied and lowest unoccupied molecular orbitals (HOMO/LUMO) levels of the dyes with respect to the conduction band edge of TiO₂ is also important.^[14,15] Quantum chemical calculations of the HOMO/LUMO energies of the dye molecules were performed by the DFT/B3LYP method with the 6-31G(d,p) basis (Gaussian 09W). The calculated HOMO energy for the Rh6G, PD1 and PD2 dyes are equal to -5.64, -6.24, -5.95 eV, respectively (Fig. 1). The energies of LUMO orbitals are equal to the -3.4, -3.34, and -3.54 eV in the same dye sequence. As can be seen from the data, the LUMO orbital energies of all selected dyes lie above the conduction band edge of TiO₂

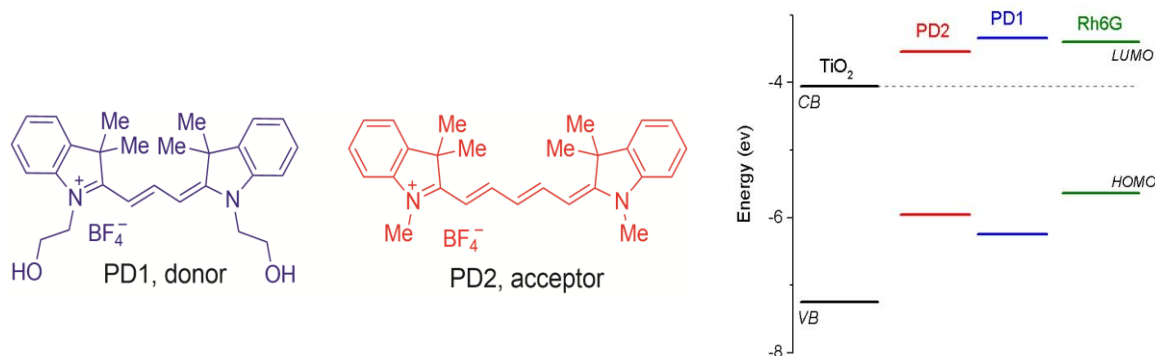


Fig. 1: Structure of PDs and band structure diagram of the compounds used.

(−4.05 eV), which makes them effective electron donors.^[16]

The dye concentration was 10^{−4} mol/L in all solutions. The TiO₂ nanoparticle pastes were prepared according to our previously published methods.^[1,17] 0.96 g of TiO₂ and 2 mL of ethylene glycol were stirred magnetically for 24 hours. Then 0.2 g of PGS was added and left for a day with constant stirring at 120 °C. The prepared pastes were deposited onto the surface of glass substrates or FTO by the doctor-blading method. The films were left to relax in air for 3 min, dried at 125 °C (6 min) and stepwise annealed in the temperature range from 175 to 500 °C (in steps of 175 °C). Next, the dyes were adsorbed onto the prepared samples by spreading 300 μL of dye solutions or donor-acceptor mixtures.

To study the plasmon effect of metal NPs, Ag@TiO₂ core@shell NPs were synthesized according to the method.^[18] The concentrations of core@shell NPs in TiO₂ film were 0.5, 1 and 2 wt%. The core diameter and the thickness of the semiconductor shell were estimated from dynamic light scattering data from Nano S90 analyser (Malvern). The diameter of core was 25±7 nm, and after the synthesis of TiO₂ shell, the average diameter was 35±7 nm (Fig. 2). Thus, the thickness of the semiconductor shell is 5±3.5 nm, which corresponds to the optimal distance for registration of plasmon-enhanced signals according to the studies.^[19,20] SEM images confirmed these results (JEM-2100F, 200 kV, Jeol), and EDA analysis of the obtained Ag@TiO₂ NPs showed the patterns of Ag and TiO₂ (Fig. 2).

Absorbance spectra were measured with a Cary 300 spectrophotometer, and fluorescence spectra were obtained with a Cary Eclipse spectrofluorimeter (Agilent Technologies). Lifetimes of donor and acceptor fluorescence of the films were determined using the TCSPC system (Becker & Hickl). Fluorescence lifetimes were estimated from the decay kinetics analyzed with the SPCImage software (Becker & Hickl) upon the excitation at λ_{exc}=488 nm.

The intensity of luminescence decay was fitted using Eq. (1):

$$I(t) = \sum_{i=1}^n \alpha_i \exp(-t/\tau_i) \quad (1)$$

where τ_i is the fluorescence lifetime, α_i is the amplitude or contribution fraction of the i-th component (∑α_i=1,0).

The energy transfer efficiency of the E_{ET} was estimated using Eq. (2):^[11,21]

$$E_{ET} = 1 - \frac{\tau_D}{\tau_{0D}} \quad (2)$$

where τ_D and τ_{0D} are the average fluorescence lifetime of the donor without and in the presence of the acceptor.

Solar cells were prepared and assembled according to the procedure described in Refs.[1, 3, 22] Doping of titanium dioxide films with dye molecules was carried out by immersing the prepared electrodes in the dye solution for 24 h, followed by washing with ethanol and drying for 2-2.5 h at 60 °C. Measurements of the current-voltage characteristics (I-V) of dye-sensitized solar cells were performed with a Solar Cell Tester (CT50AAA, Photo Emission Tech. Inc.) under AM1.5 illumination. The fill factor (FF) and the efficiency of conversion of light into electrical energy (η) were evaluated using Eqs. (3) and (4):

$$FF = \frac{(I_{max} \cdot V_{max})}{I_{sc} V_{oc}} \quad (3)$$

$$\eta = \frac{FF \cdot I_{sc} \cdot V_{oc}}{P_{in}} \cdot 100\% = \frac{P_{cell}}{P_{in}} \quad (4)$$

where I_{max}, V_{max} are the values of maximum current and voltage at the maximum of power production generated by the cell, I_{sc}, V_{oc} are the values of short-circuit current and open-circuit voltage, and P_{in} is the power of incident radiation.

3. Results and discussion

The absorption spectra of the donors and acceptors are shown in Fig. 3. The spectral overlap integral between the donor fluorescence and acceptor absorption is equal to 9.12·10^{−13} M^{−1} cm³ for the Rh6G-PD2 pair and 6.25·10^{−13} M^{−1} cm³ for the PD1-PD2 pair.

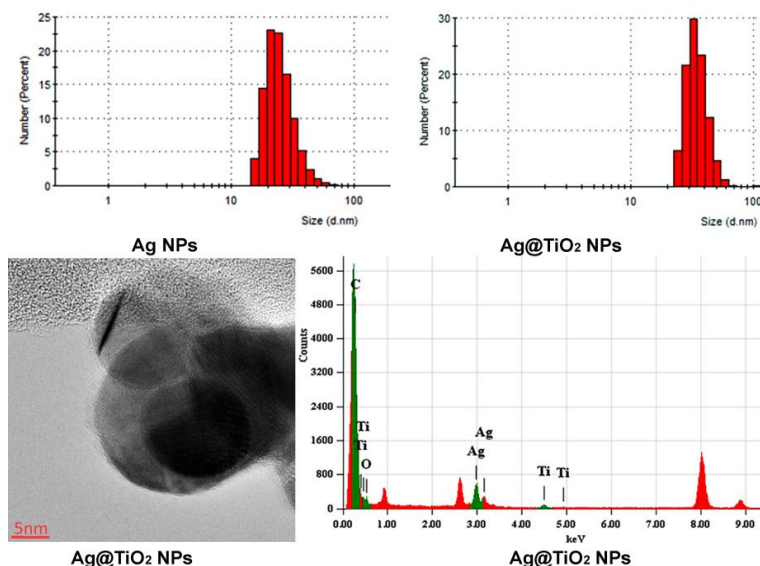


Fig. 2: Size distribution of Ag and Ag@TiO₂ NPs, TEM image and EDA spectra of Ag@TiO₂ NPs.

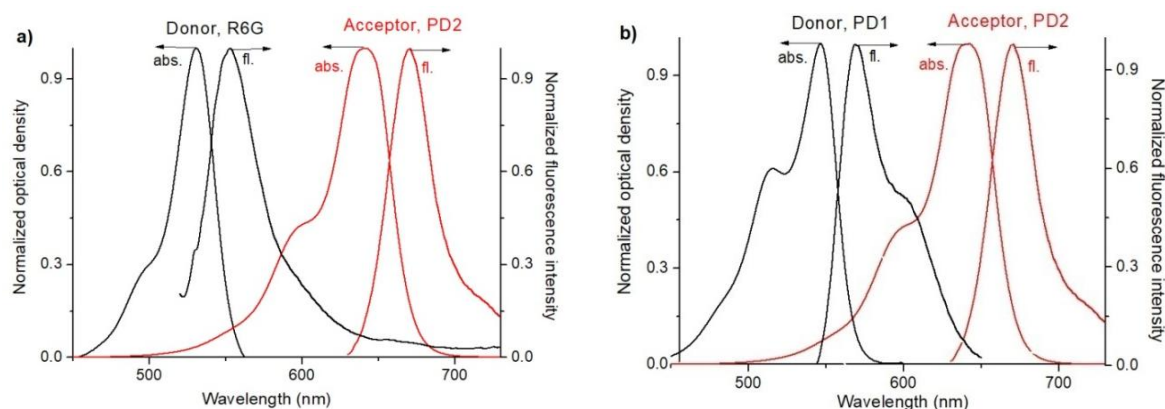


Fig. 3: Normalized absorption and fluorescence spectra of donors and acceptor of energy in ethanol solutions (10^{-5} mol/L) for Rh6G-PD2 (a) and PD1-PD2 (b) pairs.

Table 1: Characterisation of absorption, fluorescence spectra and mean lifetime τ of dyes on the TiO_2 surface without and in the presence of Ag@TiO_2 NPs of different concentrations.

Ag@TiO_2 NPs concentration (wt%)	$^{abs}\lambda_{max}$ (nm)	D	$^{fl}\lambda_{max}$ (nm)	I (a.u.)	I/I ₀	τ (ns)
Rh6G						
0%	532	0.08	550	500	–	0.83
0.5%	532	0.082	550	520	1.04	0.79
1%	532	0.083	550	530	1.06	0.74
2%	532	0.085	550	490	0.98	0.80
PD1						
0%	552	0.018	570	78	–	0.61
0.5%	552	0.020	570	85	1.09	0.60
1%	552	0.022	570	100	1.28	0.59
2%	552	0.015	570	79	1.01	0.59
PD2						
0%	640	0.09	660	430	–	0.41
0.5%	640	0.10	660	500	1.16	0.40
1%	640	0.13	660	650	1.51	0.39
2%	640	0.11	660	550	1.28	0.39

The influence of the plasmonic effect of Ag@TiO_2 NPs on the spectral and luminescence properties of the neat donor and acceptor dyes was investigated. It was found that the addition of Ag NPs did not alter the shape or position of the absorption and fluorescence bands. The maxima of the absorption and fluorescence spectra of Rh6G in TiO_2 films are at 530 and 550 nm, respectively (Table 1). The addition of Ag@TiO_2 NPs resulted in a 6% increase in both the optical density and fluorescence intensity of the dye. In the case of PD1, the optical density changed by approximately 20%, and the maximum intensity exhibited a 28% growth in the presence of Ag@TiO_2 NPs.

For the dye PD2, the corresponding values were 44% and 51%, respectively. Measurements of the fluorescence decay kinetics of the considered dyes showed that the luminescence lifetime (Eq. (1)) for all three dyes changes slightly (within 3–5%) in the presence of plasmon NPs (Fig. 4 and Table 1). The optimal concentration of Ag@TiO_2 NPs, at which the greatest plasmon effect was registered, was 1 wt% of core@shell NPs. The observed increase in the fluorescence intensity of dyes on the surface of TiO_2 indicates an enhancement of the radiative

decay rate of excited dye molecules near plasmonic NPs. The plasmon effect also increases the excitation rate of dye molecules, as confirmed by the increase in the optical density of dyes in films with the addition of core@shell NPs.^[19,23]

For the FRET study, donor-acceptor (DA) pairs were excited in the absorption band of the donor of energy (D) ($\lambda_{exc}=488$ nm). In the case of Rh6G-PD2 DA pair, measurements showed that the addition of acceptor (A) resulted in a quenching of the fluorescence intensity of Rh6G (Fig. 4a). The fluorescence lifetime of the donor in the presence of the acceptor decreased by almost 55% (Table 2). At the same time, a band appeared in the red region of the spectrum that coincides spectrally with the emission spectrum of the A. At direct excitation of A films at $\lambda_{exc}=488$ nm, their fluorescence was not registered.

Consequently, the observed fluorescence in the region of 600–750 nm with a maximum at 660 nm refers to the sensitised luminescence of PD2 molecules, resulting from FRET from S_1 -excited molecules of Rh6G to the A molecules in the ground state. The fluorescence duration of the A molecules in this case has a value close to the lifetime of D molecules in the

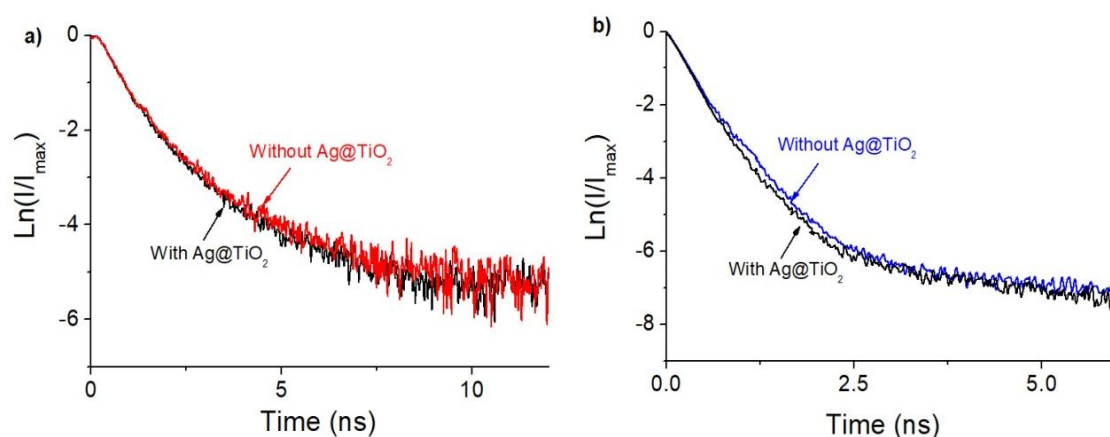


Fig. 4: Fluorescence decay kinetics of Rh6G (a) and PD1 (b) on the TiO₂ surface without and in the presence of Ag@TiO₂ NPs (1 wt%).

Table 2: Fluorescence lifetimes of donor of energy (D) (τ_D) and sensitized fluorescence of acceptor (τ_A) on the surface of TiO₂ films ($\lambda_{exc}=488$ nm), efficiency (E_{ET}) and rate constant (k_{ET}) of FRET at different concentrations of Ag@TiO₂ NPs.

Sample	E_{ET}	τ_D (ns)	τ_A (ns)	$k_{ET} \cdot 10^9$ (s ⁻¹)	k_{ET}/k_{ET}^{pl}
Rh6G–PD2					
Neat D	–	0.80	–	–	–
DA+Ag@TiO ₂ , 0 wt%	0.55	0.36	0.45	1.53	–
DA+Ag@TiO ₂ , 0.5 wt%	0.64	0.29	0.31	2.22	1.45
DA+Ag@TiO ₂ , 1 wt%	0.68	0.26	0.38	2.66	1.74
DA+Ag@TiO ₂ , 2 wt%	0.59	0.32	0.34	1.80	1.18
PD1–PD2					
Neat D	–	0.58	–	–	–
DA+Ag@TiO ₂ , 0 wt%	0.21	0.46	0.38	0.46	–
DA+Ag@TiO ₂ , 0.5 wt%	0.34	0.38	0.23	0.88	1.94
DA+Ag@TiO ₂ , 1 wt%	0.60	0.23	0.37	2.59	5.64
DA+Ag@TiO ₂ , 2 wt%	0.34	0.38	0.31	0.89	1.94

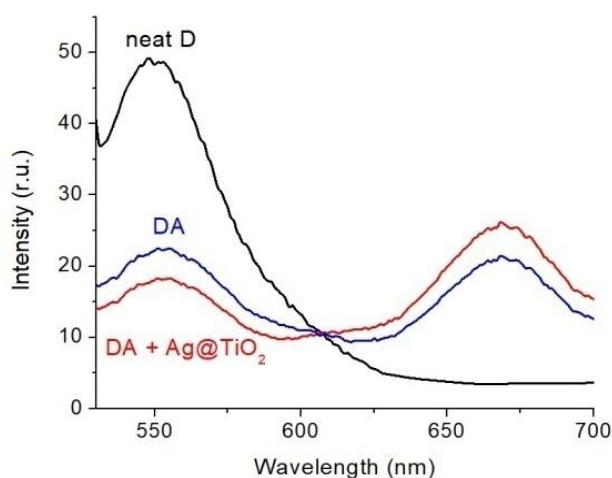


Fig. 5: Fluorescence spectra of Rh6G (D) and DA pair Rh6G–PD2 on TiO₂ surface without and in the presence of Ag@TiO₂ NPs (1 wt%), ($\lambda_{exc}=488$ nm).

excited state. The efficiency of energy transfer E_{ET} , estimated from the change in the D fluorescence lifetimes (Eq. (2)), is equal to 0.54. In the case of the PD1-PD2 pair, similar results were obtained. In the presence of acceptor molecules, the PD1 lifetime was reduced by 26% from the initial lifetimes of PD1.

The energy transfer efficiency for PD1-PD2 pair was equal to 0.21.

When comparing the energy transfer efficiency for the two donor-acceptor pairs, it can be seen that the E_{ET} value is almost twice as high for the Rh6G donor compared to PD1. This is a consequence of the smaller value of the overlap integral for the second pair compared to the first one.^[24]

In the presence of Ag/TiO₂ NPs, an increase in the efficiency of energy transfer from donor molecules to the acceptor is observed (Fig. 5). The optimal concentration of Ag/TiO₂ NPs, for maximal energy transfer efficiency is 1 wt%, which coincides with the concentration at which the highest enhancement in luminescent properties of the studied dyes was obtained.

Thus, it can be seen that FRET efficiency increases in the presence of silver NPs (Table 2). This indicates a direct effect of LPR on the energy transfer rate constant k_{ET} . The k_{ET} was evaluated according to the method.^[11,21] The greatest increase in the energy transfer rate constant occurs in the DA pair including only PDs (5.6-fold at 1 wt% Ag@TiO₂ NPs). At the same time, the value of k_{ET} for the Rh6G-PD2 pair was increased only 1.7 times. So, it can be concluded that the increase in the energy transfer efficiency is a consequence of

Table 3: Photovoltaic parameters of solar cells sensitized by DA pairs and individual dyes without and in the presence of Ag@TiO₂ NPs (1 wt%). The FF and η were calculated with Eqs. (3) and (4), correspondingly.

Sample	$I_{sc} \pm 0.0007$ (mA/cm ²)	$V_{oc} \pm 0.03$ (mV)	FF ± 0.001	$\eta \pm 0.004$ (%)	$R_{series} \pm 0.004$ (kOhm)	$R_{shunt} \pm 0.007$ (kOhm)
Rh6G						
TiO ₂	0.04	206	0.46	0.038	1.58	7.74
Ag@TiO ₂	0.05	234	0.46	0.054	1.10	7.65
PD1						
TiO ₂	0.28	352	0.18	0.180	2.69	1.39
Ag@TiO ₂	0.67	403	0.12	0.320	1.29	0.760
PD2						
TiO ₂	0.06	215	0.57	0.060	3.43	3.48
Ag@TiO ₂	0.04	246	0.56	0.070	2.99	2.34
Rh6G+PD1						
TiO ₂	0.07	224	0.35	0.055	1.08	3.75
Ag@TiO ₂	0.07	328	0.40	0.092	1.03	3.58
PD1+PD2						
TiO ₂	0.4	441	0.20	0.350	4.29	1.17
Ag@TiO ₂	0.66	445	0.16	0.670	3.82	0.76

the plasmon effect of core@shell NPs on the rate constant of FRET from D to A molecules. The greatest influence of LPR on processes with low energy transfer efficiency is a known fact.^[11]

Next, the photovoltaic parameters of the prepared DSSCs sensitized by individual donors, acceptors, and donor-acceptor mixtures were measured. In all the solar cells, the concentration of Ag@TiO₂ NPs was the same and was equal to 1 wt%, since the maximum values of k_{ET} rate and dye fluorescence intensity were obtained at this concentration. The results showed (Table 3) that in the presence of Ag@TiO₂ NPs, an increase in the efficiency (η) of all kinds of solar cells was registered. The efficiency gain for the cell sensitized only with Rh6G is 42%, with PD1 is 77%, and with PD2 is 10%. When DA pairs were used, the increase of η for the Rh6G-PD2 pair is 67%, whereas for PD1-PD2, this parameter was increased by 91%.

In order to find out how exactly plasmonic NPs affect on the growth of the efficiency of solar cells – through the effect on FRET or due to the expansion of the light-harvesting of the cell, measurements of the spectral sensitivity of the prepared cells were carried out (Fig. 6). The results showed that the spectral sensitivity curves of the solar cells coincide with the absorption spectra of the dye molecules. The addition of Ag@TiO₂ NPs to the semiconductor film results in the expansion of the spectral sensitivity into the blue wavelength region with a maximum at 420-430 nm. For solar cells, sensitized by DA solutions, the sensitivity spectrum displayed the absorption bands of the donor, acceptor, and plasmon NPs in their presence in the film.

From the data obtained, it can be concluded that for the Rh6G-PD2 pair, the increase in the solar cell efficiency is predominantly due to the broadening of the spectral sensitivity of the semiconductor film upon doping with Ag/TiO₂ NPs. In

contrast, the efficiency improvement in the PD1-PD2 pair results from both increased light-harvesting efficiency and plasmonic enhancement of FRET from D to A.

Additionally, the increase in the efficiency of DSSCs sensitized by DA pairs and individual dyes may be a consequence of the modification of the electrophysical parameters of TiO₂ films when plasmon core/shell NPs were added to them (Table 3). As can be seen from the obtained data, the values of electrical resistances R_{series} and R_{shunt} in all cells were decreased in the presence of plasmon NPs.

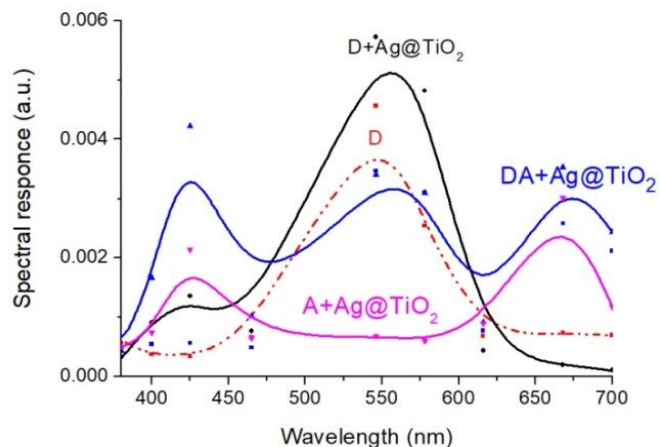


Fig. 6: Spectral sensitivity curves of solar cells sensitized with dyes PD1 (D) and PD2 (A), as well as the DA pair PD1-PD2 without (red curve) and in the presence of Ag@TiO₂ NPs (other curves).

4. Conclusion

The obtained results showed that the combination of LPR of Ag NPs and FRET can significantly enhance the sensitization efficiency of solar cells. It is shown that in DA pairs based on rhodamine and polymethine dyes, as well as in a pair of

cationic indopolycarbocyanines adsorbed on the surface of TiO₂ semiconductor films, FRET is effectively carried out. The energy transfer efficiency is higher for the first DA pair ($E_{ET}=0.55$) than for the second ($E_{ET}=0.21$). In the presence of Ag/TiO₂ NPs, an increase in the efficiency of energy transfer from D molecules to the A molecules was observed. The optimal concentration of Ag/TiO₂ NPs, at which the greatest enhancement of the transfer efficiency was registered, is equal to 1 wt%. The increase of E_{ET} is related to the direct influence of LPR on the rate constant of energy transfer k_{ET} . The largest increase in the energy transfer rate occurs in the DA pair of polymethine dyes (by a factor of 5.6 at a concentration of Ag@TiO₂ NPs equal to 1 wt%). At the same time, the energy transfer rate in the Rh6G-PD2 pair was increased only 1.7 times. The synergetic effect of FRET and LPR of Ag@TiO₂ NPs led to an improvement in the efficiency of all investigated solar cells. The increase in η of a solar cell with plasmon NPs sensitised by the Rh6G-PD2 pair was equal to 67%, whereas for PD1-PD2, this parameter was increased by 91%. Investigations of the spectral sensitivity of the cells have shown that the increase in the efficiency of the photovoltaic cell is not only due to the increase in the light-harvesting efficiency of the cell, but also due to the plasmon enhancement of the FRET efficiency from D to A. Also, the improvement of the electrophysical parameters of the investigated solar cells cannot be excluded. Overall, these findings indicate that the combined usage of LPR and FRET holds promise for improving the performance of DSSCs sensitized with metal-free dyes.

Acknowledgements

This work was supported by the Science Committee of the Ministry of Science and Higher Education of the Republic of Kazakhstan [Grant No. AP19680241].

Conflict of Interest

There is no conflict of interest.

Supporting Information

Not applicable.

References

- [1] N. Ibrayev, E. Seliverstova, N. Nuraje, A. Ishchenko, FRET-designed dye-sensitized solar cells to enhance light harvesting, *Materials Science in Semiconductor Processing*, 2015, **31**, 358-362, doi: 10.1016/j.mssp.2014.12.006.
- [2] N. Ibrayev, E. Seliverstova, A. Aimukhanov, T. Serikov, Role of energy transfer in conversion of light to electric energy, *Molecular Crystals and Liquid Crystals*, 2014, **589**, 202-208, doi: 10.1080/15421406.2013.872827.
- [3] R. Ramanarayanan, S. Swaminathan, Improving efficiency of natural dye sensitized solar cell using FRET mechanism, *Materials Today: Proceedings*, 2022, **60**, 1125-1129, doi: 10.1016/j.matpr.2022.02.285.
- [4] M. T. Efa, J. Huang, T. Imae, Cascade Förster resonance energy transfer studies for enhancement of light harvesting on dye-sensitized solar cells, *Nanomaterials*, 2022, **12**, 4085, doi: 10.3390/nano12224085.
- [5] W. Li, J. Li, M. Sun, Physical mechanisms on FRET and ICT for efficient Y6: PM6 as bulk heterojunction active layers, *Physical Chemistry Chemical Physics*, 2023, **25**, 9807-9816, doi: 10.1039/d3cp00819c.
- [6] T. Wang, X. Wang, R. Yang, C. Li, Recent advances in ternary organic solar cells based on Förster resonance energy transfer, *Solar RRL*, 2021, **5**, 2100496, doi: 10.1002/solr.202100496.
- [7] B. Zhang, P. Zhao, L. J. Wilson, J. Subbiah, H. Yang, P. Mulvaney, D. J. Jones, K. P. Ghiggino, W. W. H. Wong, High-performance large-area luminescence solar concentrator incorporating a donor-emitter fluorophore system, *ACS Energy Letters*, 2019, **4**, 1839-1844, doi: 10.1021/acsenergylett.9b01224.
- [8] C. Tummelshammer, M. Portnoi, S. A. Mitchell, A.-T. Lee, A. J. Kenyon, A. B. Tabor, I. Papakonstantinou, On the ability of Förster resonance energy transfer to enhance luminescent solar concentrator efficiency, *Nano Energy*, 2017, **32**, 263-270, doi: 10.1016/j.nanoen.2016.11.058.
- [9] B. Zhang, G. Lyu, E. A. Kelly, R. C. Evans, Förster resonance energy transfer in luminescent solar concentrators, *Advanced Science*, 2022, **9**, 2201160, doi: 10.1002/advs.202201160.
- [10] P. Roy, A. S. Sury, P. P. Pillai, Resonance energy transfer in electrostatically assembled donor-acceptor system based on blue-emitting InP quantum dots, *Chemical Physics Impact*, 2023, **7**, 100334, doi: 10.1016/j.chphi.2023.100334.
- [11] N. Ibrayev, E. Seliverstova, N. Zhumabay, D. Temirbayeva, Plasmon effect in the donor-acceptor pairs of dyes with various efficiency of FRET, *Journal of Luminescence*, 2019, **214**, 116594, doi: 10.1016/j.jlumin.2019.116594.
- [12] M. Lunz, V. A. Gerard, Y. K. Gun'ko, V. Lesnyak, N. Gaponik, A. S. Susha, A. L. Rogach, A. L. Bradley, Surface plasmon enhanced energy transfer between donor and acceptor CdTe nanocrystal quantum dot monolayers, *Nano Letters*, 2011, **11**, 3341-3345, doi: 10.1021/nl201714y.
- [13] K. Afroz, R. Dupre, N. Nuraje, Nanomaterials for water splitting, 21st Century Nanoscience - A Handbook, Industrial Applications, CRC Press, Boca Raton, 2020, 228-256, ISBN: 9780429351594.
- [14] J. Li, H. Guo, Y. Zhong, Y. Li, P. Song, Theoretical study of novel xanthene-linked L-(D- π -a)₂-type double-anchored dyes for dye-sensitized solar cells: Effects of π bridge length and TiO₂ adsorption pattern, *Computational and Theoretical Chemistry*, 2025, **1246**, 115125, doi: 10.1016/j.comptc.2025.115125.
- [15] B. Baptayev, S.-M. Kim, B. Bolatbek, S. H. Lee, M. P. Balanay, Effect of π -spacer length in novel xanthene-linked l-(D- π -a)₂-type dianchoring dyes for dye-sensitized solar cells, *ACS Applied Energy Materials*, 2022, **5**, 6764-6771, doi: 10.1021/acsaem.2c00384.
- [16] J. I. Fujisawa, T. Eda, M. Hanaya, Comparative study of conduction-band and valence-band edges of TiO₂, SrTiO₃, and BaTiO₃ by ionization potential measurements, *Chemical Physics Letters*, 2017, **685**, 23-26, doi: 10.1016/j.cplett.2017.07.031.

- [17] N. Ibrayev, E. Seliverstova, G. Omarova, A. Ishchenko, Sensitization of TiO₂ by merocyanine dye in the presence of plasmon nanoparticles, *Materials Today: Proceedings*, 2022, **49**, 2464-2468, doi: 10.1016/j.matpr.2020.11.424.
- [18] D. A. Afanasyev, N. K. Ibrayev, T. M. Serikov, A. K. Zeinidenov, Effect of the titanium dioxide shell on the plasmon properties of silver nanoparticles, *Russian Journal of Physical Chemistry A*, 2016, **90**, 833-837, doi: 10.1134/s0036024416040026.
- [19] P. Anger, P. Bharadwaj, L. Novotny, Enhancement and quenching of single-molecule fluorescence, *Physical Review Letters*, 2006, **96**, 113002, doi: 10.1103/physrevlett.96.113002.
- [20] N. K. Ibrayev, E. V. Seliverstova, R. R. Valiev, A. E. Kanapina, A. A. Ishchenko, A. V. Kulinich, T. Kurten, D. Sundholm, Influence of plasmons on the luminescence properties of solvatochromic merocyanine dyes with different solvatochromism, *Physical Chemistry Chemical Physics*, 2023, **25**, 22851-22861, doi: 10.1039/d3cp03029f.
- [21] J. Zhang, Y. Fu, J. R. Lakowicz, Enhanced Förster resonance energy transfer (FRET) on a single metal particle, *The Journal of Physical Chemistry C*, 2007, **111**, 50-56, doi: 10.1021/jp062665e.
- [22] N. Ibrayev, G. Omarova, E. Seliverstova, A. Ishchenko, N. Nuraje, Plasmonic effect of Ag nanoparticles on polymethine dyes sensitized titanium dioxide, *Engineered Science*, 2021, **14**, 69-77, doi: 10.30919/es8d1168.
- [23] S. Schlücker, Surface enhanced Raman spectroscopy: Analytical, biophysical and life science applications, Wiley-VCH Verlag GmbH and Co. KGaA, Weinheim, 2011, 354, ISBN: 9783527325672.
- [24] E. V. Seliverstova, D. A. Temirbayeva, N. K. Ibrayev, A. A. Ishchenko, Plasmon effect of Ag nanoparticles on Förster resonance energy transfer in a series of cationic polymethine dyes, *Theoretical and Experimental Chemistry*, 2019, **55**, 115-124, doi: 10.1007/s11237-019-09602-9.

directly from the copyright holder. To view a copy of this license, visit <http://creativecommons.org/licenses/by/4.0/>.

©The Author(s) 2025

Publisher's Note: Engineered Science Publisher remains neutral with regard to jurisdictional claims in published maps and institutional affiliations.

Open Access

This article is licensed under a Creative Commons Attribution 4.0 International License, which permits the use, sharing, adaptation, distribution and reproduction in any medium or format, as long as appropriate credit to the original author(s) and the source is given by providing a link to the Creative Commons license and changes need to be indicated if there are any. The images or other third-party material in this article are included in the article's Creative Commons license, unless indicated otherwise in a credit line to the material. If material is not included in the article's Creative Commons license and your intended use is not permitted by statutory regulation or exceeds the permitted use, you will need to obtain permission